Biol. Cell (2017) **109,** 81–93 DOI: 10.1111/boc.201600042

Review

The integrative role of cryo electron microscopy in molecular and cellular structural biology

Igor Orlov*†‡§, Alexander G. Myasnikov*†‡§, Leonid Andronov*†‡§, S. Kundhavai Natchiar*†‡§, Heena Khatter*†‡§[2], Brice Beinsteiner*†‡§, Jean-François Ménétret*†‡§, Isabelle Hazemann*†‡§, Kareem Mohideen*†‡§, Karima Tazibt*†‡§, Rachel Tabaroni*†‡§, Hanna Kratzat*†‡§, Nadia Djabeur*†‡§, Tatiana Bruxelles*†‡§, Finaritra Raivoniaina*†‡§, Lorenza di Pompeo*†‡§, Morgan Torchy*†‡§, Isabelle Billas*†‡§, Alexandre Urzhumtsev*†‡§ and Bruno P. Klaholz*†‡§[1]

*Centre for Integrative Biology (CBI), Department of Integrated Structural Biology, IGBMC (Institute of Genetics and of Molecular and Cellular Biology), Illkirch, France, †Centre National de la Recherche Scientifique (CNRS) UMR 7104, Illkirch, France, ‡Institut National de la Santé et de la Recherche Médicale (INSERM) U964, Illkirch, France, and §Université de Strasbourg, Strasbourg, France

After gradually moving away from preparation methods prone to artefacts such as plastic embedding and negative staining for cell sections and single particles, the field of cryo electron microscopy (cryo-EM) is now heading off at unprecedented speed towards high-resolution analysis of biological objects of various sizes. This 'revolution in resolution' is happening largely thanks to new developments of new-generation cameras used for recording the images in the cryo electron microscope which have much increased sensitivity being based on complementary metal oxide semiconductor devices. Combined with advanced image processing and 3D reconstruction, the cryo-EM analysis of nucleoprotein complexes can provide unprecedented insights at molecular and atomic levels and address regulatory mechanisms in the cell. These advances reinforce the integrative role of cryo-EM in synergy with other methods such as X-ray crystallography, fluorescence imaging or focussed-ion beam milling as exemplified here by some recent studies from our laboratory on ribosomes, viruses, chromatin and nuclear receptors. Such multi-scale and multi-resolution approaches allow integrating molecular and cellular levels when applied to purified or *in situ* macromolecular complexes, thus illustrating the trend of the field towards cellular structural biology.

Introduction

The key event in cryo electron microscopy (cryo-EM) has been the introduction of cryo methods that allow preserving the biological sample in a hydrated and functional state (Dubochet et al., 1988). One of the reasons for the importance of cryo methods is that artefacts due to sample dehydration, fixation, adsorption and staining can be avoided, thus allowing the sample to be observed in a functionally relevant state. Sample preservation is thus an advantage of cryo methods that is worth considering both for single particle analysis of complexes extracted from the cellular context and the analysis of cell sections (*i.e.* in contrast to plastic embedding, fixation etc.). The second good reason to use cryo methods is that they allow performing high-resolution analysis, whereas conventional methods intrinsically limit the

[1]To whom correspondence should be addressed (email: klaholz@igbmc.fr)
[2]Present address: European Molecular Biology Laboratory (EMBL), Structural and Computational Biology Unit, Meyerhofstrasse 1, 69117 Heidelberg, Germany.

Key words: cryo electron microscopy, cryo electron tomography, Crystallography, Super-resolution microscopy, Structural biology.

Abbreviations: cryo-EM, cryo electron microscopy; cryo-ET, cryo electron tomography; CCD, charge-coupled device; CMOS, complementary metal oxide semiconductor; DDD, direct detection device; DQE, detective quantum efficiency; EcR, ecdysone receptor; FIB, focussed-ion beam; FRISBI, French Infrastructure for Integrated Structural Biology; Instruct, Integrated Structural Biology Infrastructure for Europe; kDa, kilo Dalton; MSA, multi-variate statistical analysis; mRNA, messenger RNA; rRNA, ribosomal RNA; SEM, scanning electron microscopy; SMLM, single-molecule localisation microscopy; tRNA, transfer RNA; 2D, two dimensional; 3D, three dimensional.

attainable resolution. This second aspect was rather clear early on when cryo techniques were introduced in the field, as illustrated by the stunning amount of molecular structures visible by eye on cryo-EM images of various samples such as viruses, chromatin and ribosomes (Dubochet et al., 1988). However, it became obvious that the main limitation in seeing high-resolution details and being able to reconstruct them computationally in three dimensions (3D) was the ability to record appropriate images with good contrast and at the same time preserve the high-resolution information (*i.e.* avoid defocussing the microscope too much). For decades, the recording medium was photographic film (negatives, *e.g.* SO-163 from Kodak) which had the advantage of being able to record a large field of the specimen ($\sim 8 \times 10$ cm film support size) and at high resolution (grain size around 10 μm), and have a good detective quantum efficiency (DQE) as compared with charge-coupled devices (CCDs). Nevertheless, CCDs had the advantage of direct data acquisition, that is no need for digitising negatives on a scanning device, an aspect that facilitates automation of image processing. However, the strongest and latest breakthrough is the introduction of direct electron detectors (based on a complementary metal oxide semiconductor (CMOS) detector with a direct detection device (DDD) sensor) which have much higher sensitivity than film or CCD thanks to their direct measurement of electron events, requiring no amplification of the signal nor fibre or lens optics (*e.g.* CCDs operate through an electron to light conversion by a scintillator followed by coupled fibre optics). Latest-generation variants of these direct electron detectors comprise (i) back-thinning of the silicon chip to avoid multiple electron scattering events, (ii) counting-mode to measure individual electron events at high read-out speeds (tens to hundreds of frames per second), (iii) localisation of the electron impact position with sub-pixel precision (*i.e.* super-resolution mode). Specific characteristics of these cameras have been described (McMullan et al., 2009; Ruskin et al., 2013; McMullan et al., 2014; Kuijper et al., 2015; Spear et al., 2015) and include an overall high DQE across the entire frequency range, wherein the particularly increased amplitudes in the low frequency range provide a much improved image contrast. An additional feature is the high read-out speed that allows dose fractionation and movie processing (Brilot et al., 2012; Campbell et al., 2012; Li et al., 2013; Veesler et al., 2013; Allegretti et al., 2014; Scheres, 2014), that is beam-induced specimen drift can be motion-corrected by aligning a series of low-dose images taken on one given area of the specimen (Kunath et al., 1984); in addition, sub-frames with optimised dose can be selected for image processing (exposure filtering; Grant et al., 2015). It is these major technological developments of new-generation detectors that have recently introduced a 'revolution in resolution' in the cryo-EM field, analogous to the impact of the Pilatus & Eiger pixel detectors in the field of X-ray crystallography (Broennimann et al., 2006; Rajendran et al., 2011; Casanas et al., 2016). This has greatly contributed to a strong increase of the amount of structures determined by cryo-EM within the last few years (Figure 1).

If the sample permits it, such cameras in principle allow – in synergy with advanced image processing informatics tools – to determine 3D structures in the 3 Å resolution range. Such resolution values allow building and refining atomic models against the cryo-EM maps. To illustrate this in more detail, we will now provide some examples of recent high-resolution cryo-EM analysis from projects of our laboratory (Figure 2) and we will discuss the integrative role of cryo-EM in synergy with other complementary methods. This reflects the general trend of the field towards cellular structural biology which relies more and more on multi-resolution and multi-scale approaches to address the molecular and cellular organisation of living cells (Figure 3).

Single particle cryo-EM analysis

The strength of current cryo-EM relies on the combination of cutting-edge instrumentation (high-resolution cryo electron microscopes equipped with direct electron detectors, such as those made available through the European and French infrastructures Instruct and FRISBI, see https://www.structuralbiology.eu/ and http://frisbi.eu/) and advanced image processing. Image processing and 3D reconstruction represent important components of modern cryo-EM because they allow getting unique and detailed 3D insights into the object of interest, much beyond a visual 2D description at low resolution. Images obtained on a transmission electron microscope are 2D projection images of the object and therefore contain all internal features of the 3D

Figure 1 | Recent increase of cryo-EM and cryo-ET studies as illustrated from the number of map depositions in the EMDB as a function of time and resolution

(**A, B**) Largely thanks to developments of high-sensitivity detectors, the year 2013 (arrow) marks a transition of the exponentially growing number of structures determined by cryo-EM or cryo-ET, that is the curve became bimodal with a steep increase in the last 4 years which is likely to continue considering the vast amount of biological objects that now become amendable to cryo-EM and cryo-ET analysis. This is also visible in the growing contribution of high-resolution cryo-EM structures over the four last years (B). The data are taken from the http://www.ebi.ac.uk/pdbe/emdb/ and http://www.rcsb.org/pdb/ websites (as of September 26, 2016).

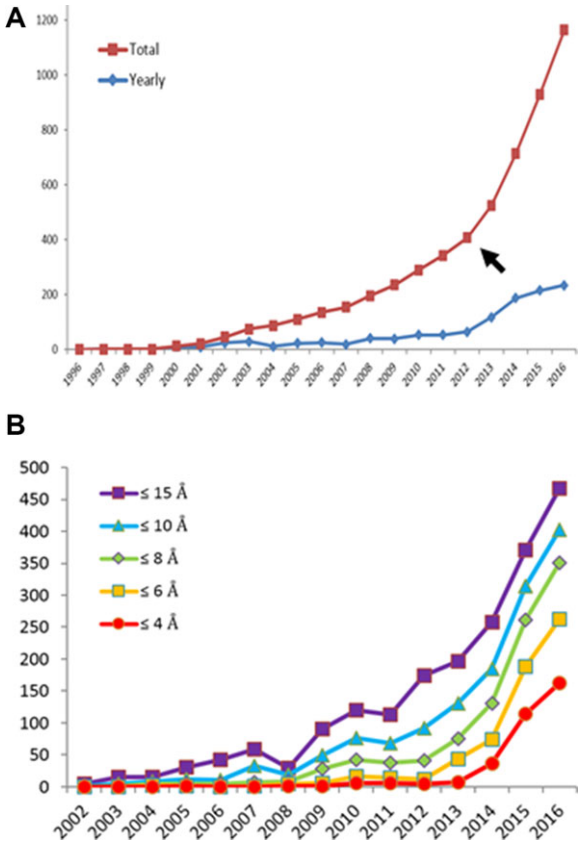

object which is seen under different orientations. Thus, reversely, a 3D map of the object can be obtained from 2D projection images by back-projection, that is the views of the 3D object seen under different orientations (viewing angles) can be combined into a single 3D reconstruction; this concept applies to both single particle cryo-EM and cryo electron tomography (cryo-ET; for detailed basics on image processing and 3D reconstruction see for example reviews by van Heel et al., 2000; Ray et al., 2003; Briggs et al., 2013; Lučič et al., 2013; Milne et al., 2013; Scheres, 2014; Carazo et al., 2015; Carroni et al., 2016). An assumption in the 3D reconstruction process is that the input images describe the same object that it is functionally, structurally and conformationally homogenous. While this is the case for a single tomogram (recorded on one single object), it is rarely the case when averaging techniques are used, that is sub-tomogram averaging and single particle reconstruction using images describing (and tentatively merging) physically different objects. Sample heterogeneity can make the interpretation of 3D maps difficult or even impossible and might significantly limit the attainable resolution of the 3D reconstruction. Therefore, methods for 3D classifications to enable structure sorting are becoming an essential tool for the high-resolution analysis of single particle cryo-EM data, allowing the simultaneous analysis of several structures that are in equilibrium with each other. Examples of these are approaches based on cross correlation analysis using reference structures (template-based supervised classification, Gao et al., 2004) or based on multivariate statistical analysis (MSA) including local variance analysis in the particle images (White et al., 2004; Klaholz et al., 2004; Orlova & Saibil, 2010), resampling and bootstrapping methods to identify flexible regions in a macromolecular complex and perform 3D classifications (Penczek et al., 2006; Simonetti et al., 2008; Fischer et al., 2010; Klaholz, 2015; Liao et al., 2015), unsupervised classification (Fu et al., 2006) and maximum-likelihood (ML) based 3D classifications (Sigworth 1998; Scheres et al., 2010; Scheres et al., 2010; Lyumkis et al., 2013). The three categories of 2D/3D classification methods thus comprise (i) template-based methods which are intrinsically reference-biased, (ii) classification based on statistical analysis using MSA and bootstrapping methods and (iii) ML-based sorting; methods (ii) and (iii) are now commonly used as they turn out to be more robust during cryo-EM image processing of variable structures. These methods start from a low-resolution identification of larger conformational changes of the macromolecule of interest and then iteratively extend towards high-resolution sorting and

Figure 2 | Examples of high-resolution cryo-EM and cryo-ET studies using direct electron detectors

(**A**) The introduction of CMOS-based direct electron detectors in the EM field has led to a 'revolution in resolution' thanks to their much increased sensitivity (as an example, here the Falcon camera from the FEI company; setup installed on the Polara and Titan Krios cryo electron microscopes at the Centre for Integrative Biology, IGBMC; available through infrastructure access at https://www.structuralbiology.eu/ and http://frisbi.eu/). (**B**) First high-resolution structure determination of the human 80S ribosome (Khatter et al., 2015). The map obtained from single particle cryo-EM image processing and 3D reconstruction (40S and 60S ribosomal subunits are labelled, the exit site tRNA is colored in red) allows visualising side-chains of amino acids and nucleic acids whose position needs to be known with precision to perform structure-based drug design (panels on the right; including a first human 80S complex with an antibiotic; Myasnikov et al., 2016). Two aspects can be highlighted there: (i) a resolution in the 3 Å range that is required to derive detailed atomic models can nowadays be obtained even for asymmetric objects, and (ii) cryo-EM has the potential to be used for structure-based drug design. (**C**) Comparison of cryo-ET reconstructions (after sub-tomogram averaging) obtained using either a CCD camera or a CMOS camera, illustrating the increased amount of structural features that can be visualised (poly-ribosome assembly, 60S and 40S ribosomal subunits are labelled in blue and yellow, respectively; Myasnikov et al., 2014). (**D**) Single particle cryo-EM reconstruction of the 1358 bacteriophage capsid (cross-section through the 3D reconstruction; Orlov et al., unpublished) in which secondary structure elements such as α-helices and residue details (side-chains; white arrow) can be visualised.

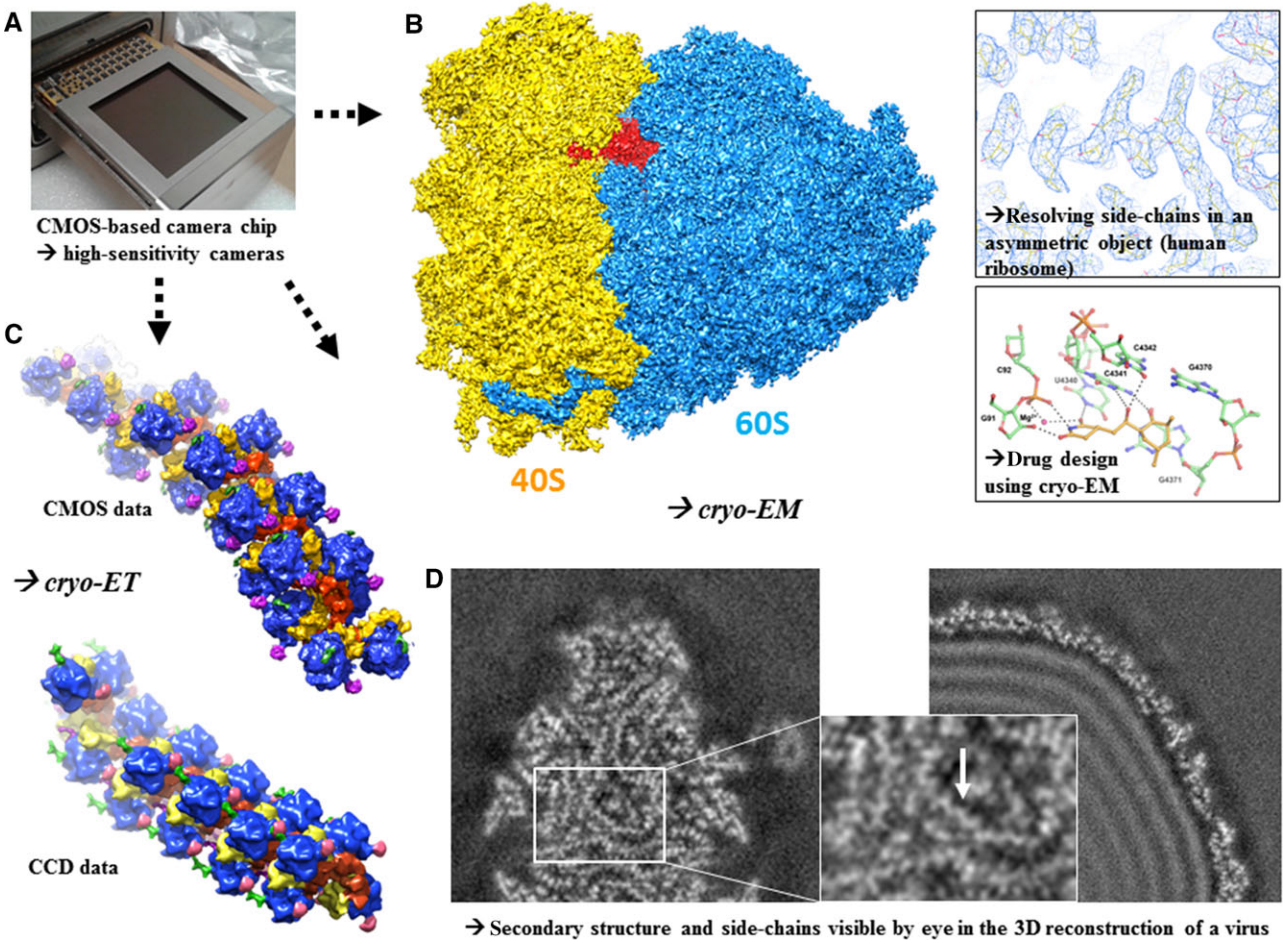

Figure 3 | Scale of things and the integrative role of cryo-EM in molecular and cellular structural biology Schematic representation of the multi-scale and multi-resolution approach in structural biology. Various examples of macromolecular complexes studied in our group are shown to illustrate the integrative role of cryo-EM/cryo-ET at the interface with complementary methods such as X-ray crystallography, NMR, SAXS (towards the molecular and atomic levels on the right) and FIB/SEM, super-resolution fluorescence microscopy (PALM, STORM/GSDIM, STED etc.) and optical/confocal microscopy (towards the cellular level on the left). Right to left: crystal structure of translation initiation factor IF2 and SAXS analysis of IF2 (Simonetti et al., 2013a), single particle cryo-EM structure of the 100 kDa nuclear receptor complex USP/EcR (Maletta et al., 2014); the structures are zoomed 4× for visualisation; middle: single particle cryo-EM analysis of the human 80S ribosome (Khatter et al., 2015) and the 1358 bacteriophage (Orlov et al., unpublished) and cryo-ET analysis of eukaryotic polyribosomes (Myasnikov et al., 2014); left: super-resolution imaging (GSDIM) of RNA polymerase (green) and histone H2B (red) and cluster analysis using new tools (Andronov et al., 2016a, 2016b); FIB/SEM analysis of HeLa cells (Orlov et al., 2015).

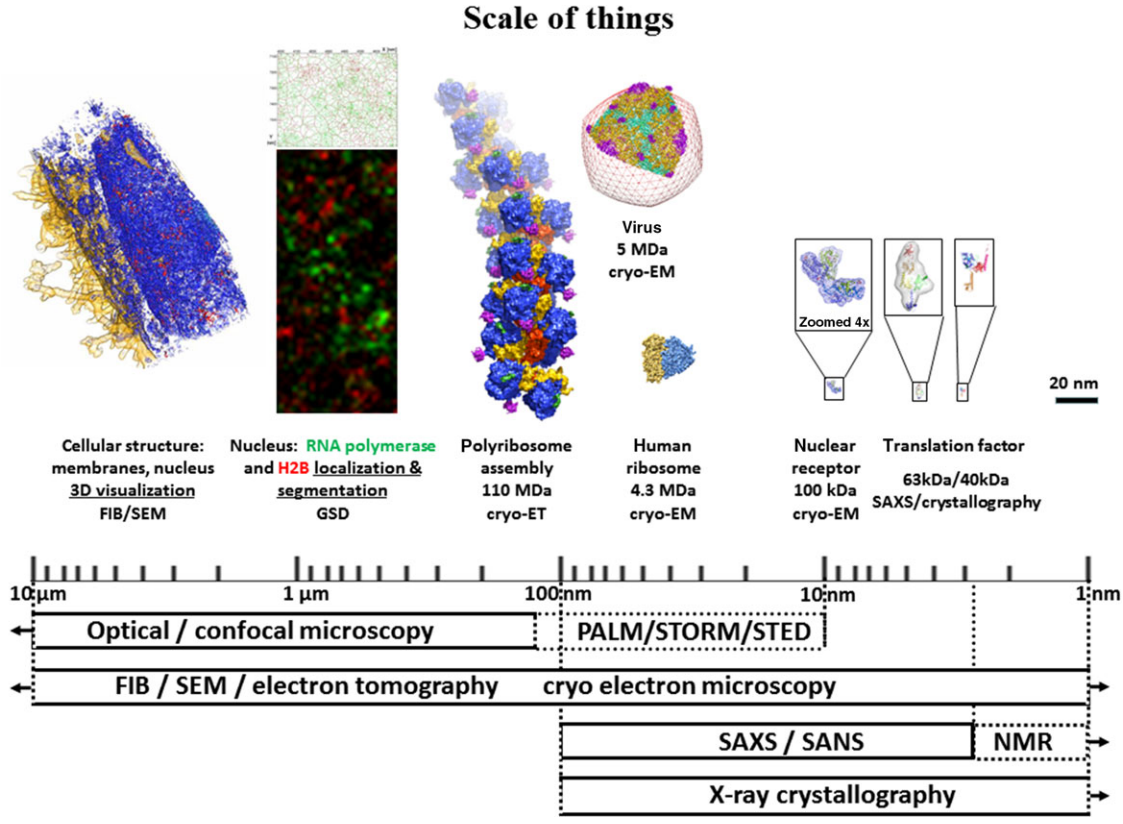

structure refinement (discussed in more detail in Klaholz, 2015).

Recent examples of high-resolution single particle cryo-EM analysis include work on various complexes such as viruses, ribosomes, proteasome, β-galactoside and so on (among many others: Chen et al., 2009; Zhang et al., 2013; Bai et al., 2013; Wong et al., 2014; Banerjee et al., 2016; Earl et al., 2016; Fischer et al., 2015; Khatter et al., 2015; Greber et al., 2015). Among the macromolecular complexes that we recently studied in our laboratory to high resolution (3 Å resolution range) using cryo-EM are the human ribosome and a virus (phage 1358); moreover, we also analysed a macromolecular assembly of poly-ribosomes by cryo-ET. These projects all benefited from the direct electron detector technology, high-resolution cryo electron microscopes and appropriate image processing (Figure 2).

Analysing the structure of the human ribosome can be considered to be the ultimate goal in structural studies of eukaryotic ribosomes, but it had to overcome the common *a priori* thinking that human

ribosomes would be too inhomogenous and difficult to analyse. In order to address this issue, we developed biochemical protocols for the high-quality preparation of human ribosomes (Khatter et al., 2014) and their high-resolution structural analysis using advanced high-resolution cryo-EM and atomic model building (Figure 2; Khatter et al., 2015). The combination of data acquisition on a DDD camera, high-resolution image processing including 3D classifications and atomic model building and refinement using tools from the field of X-ray crystallography [PHENIX (Afonine et al., 2012), Chimera (Yang et al., 2012) and Coot (Emsley et al., 2010), among other available tools (*e.g.* Buster, REFMAC, CNS etc.; Smart et al., 2012; Brown et al., 2015; Adams et al., 2013; Natchiar et al., in prep.)] allowed determining the first atomic structure of the human ribosome. In this context, it is worth noting that the procedures for atomic model building and refinement into cryo-EM maps are evolving a lot recently, illustrating a strong synergy between crystallographic methods and cryo-EM (Brown et al., 2015; Barad et al., 2015; Sobolev et al., 2015; Natchiar et al., in prep.). The structural analysis of the human ribosome enabled full integration down to the atomic level, thus providing unprecedented insights into nucleotide and amino acid side-chains which can be analysed with respect to sequence conservation using a new tool for integrated sequence and 3D structure analysis of large macromolecular complexes (Beinsteiner et al., 2015). For example, it uncovered specific molecular interactions of the 28S rRNA with the universally conserved CCA end of the tRNA in the exit site. The structure opens the possibility of studying the molecular basis of interactions of drugs with the human ribosome, as well as functional complexes with mRNA, tRNA and protein factors. A follow-up study is the first structure of a ligand complex with the human ribosome that we recently determined, highlighting the potential of the human ribosome as a drug target for protein synthesis deregulations such as cancer (proliferating cells are dependent on elevated protein synthesis rates) and illustrating the capacity of high-resolution cryo-EM for structure-based drug design studies (Figure 2; Myasnikov et al., 2016). For comparison, our previous studies of bacterial translation initiation complexes were limited to a much lower resolution (8–10 Å; Simonetti et al., 2008; Simonetti et al., 2013a,2013b; Eiler et al., 2013; Simonetti et al., 2016) but nevertheless allowed addressing the localisation of initiation factors and tRNA, thus providing a solid basis for synergies with other methods including X-ray crystallography and solution SAXS.

Another example of a high-resolution single particle cryo-EM study is our ongoing structural analysis of the capsid of the lactococcal siphophage 1358 virion. Previously, negative staining EM and cryo-EM were used to determine the structure of the different parts of this tailed bacteriophage from the *Siphoviridae* family and to assemble an overall composite structure of the phage (Spinelli et al., 2014). The building units comprise the capsid, the connector, the tail and the base-plate. The structural analysis of the capsid using high-resolution cryo-EM now provides unprecedented insights in the 3–4 Å range (refinement ongoing; Orlov et al., unpublished). The quality of the structure is illustrated by the wealth of structural details that can be seen even by eye in the cross-section of the 3D reconstruction including secondary structure elements and side-chains. Indeed, zig-zag shapes in the densities reveal α-helices and protruding densities correspond to the amino acid side-chains (Figure 2, bottom right). This highlights the fact that a resolution has been reached that is sufficient for tracing the peptide backbone and positioning side-chains from the amino acid sequence, thus allowing an atomic model refinement against the cryo-EM map. Considering that phage 1358 infects *L. lactis* strains and has some similarity to *Listeria* phages, these structural investigations may be useful for medical and agricultural implications.

Cryo-ET analysis and sub-tomogram averaging

Cryo-ET is particularly useful to analyse unique cellular structures. Rather than obtaining a 3D reconstruction from different orientational views of physically different objects like in single particle cryo-EM, it is obtained from images acquired while rotating the sample with predefined angles. The images of a tilt series can then be aligned to reconstruct a tomogram (see for example Briggs, 2013; Lučič et al., 2013; Dubrovsky et al., 2015; Asano et al., 2016). If common sub-structures exist these can be extracted as sub-tomograms, aligned and averaged to form sub-tomogram averages with an improved signal-to-noise ratio (Wan et al., 2016; Galaz-Montoya et al., 2016).

Such approaches have been used in the past to analyse, for example, the cellular structure of the nuclear pore complex (NPC), of membrane-bound ribosomes, of actin filaments in combination with segmentation tools and template-based identification of the components (Frangakis et al., 2002; Medalia et al., 2002; Beck et al., 2004; Ortiz et al., 2006). Recently, stunning insights into cellular sub-structures have been obtained (Hagen et al., 2015; Nans et al., 2015; Chang et al., 2016; Irobalieva et al., 2016; Kosinski et al., 2016; Lin et al., 2016; Mahamid et al., 2016), achieving in a first case even side-chain resolution (Schur et al., 2016) using optimised cryo-ET, sub-tomogram averaging and a new dose-symmetric tilt acquisition scheme that preserves high-resolution data more isotropically (Hagen et al., 2016). We used cryo-ET in combination with sub-tomogram averaging and molecular modelling to address the supramolecular organisation of eukaryotic polyribosomes which can form large macromolecular assemblies (Brandt et al., 2010; Myasnikov et al., 2013; Afonina et al., 2014; Myasnikov et al., 2014; Afonina et al., 2015). This allowed deriving the 3D structure of one of the largest asymmetric complexes to date (~100 MDa, comprising over 20 ribosomes on the same mRNA molecule; Myasnikov et al., 2014). The structure allowed the visualisation of the three functional parts of the polysome assembly: the central core region that forms a rather compact left-handed supramolecular helix and the more open regions that harbour the initiation and termination sites at either ends. The helical region forms a continuous mRNA channel where the mRNA strand bridges neighbouring exit and entry sites of the ribosomes and prevents the mRNA from looping between ribosomes. This structure provides unprecedented insights into protein- and RNA-mediated inter-ribosome contacts that involve conserved sites through 40S ribosomal subunits and long protruding RNA expansion segments. These findings shed new light on the molecular machinery of the ribosome and its mode of action in the cellular context. The impact of direct electron detectors is illustrated by the improved resolution of the tomograms (Figure 2). In the future, contrast-increasing phase plates may be helpful to address more of the molecular details within polysomes, possibly in combination with double tilt cryo-ET which provides 3D reconstructions with less reconstruction artefacts (Myasnikov et al., 2013; one of the first examples of single particle cryo-ET together with some other examples: Dudkina et al., 2010; Murata et al., 2010; Wang et al., 2011).

Integrative role of cryo-EM and current trends in complementary approaches

Another aspect of cryo-EM is its integrative role in multi-scale and multi-resolution approaches that integrate molecular and cellular levels by combining various structural methods such as X-ray crystallography, fluorescence imaging or focussed-ion beam milling as exemplified here by some recent studies from our laboratory on ribosomes, viruses, chromatin and nuclear receptors (Figure 3). An important consideration is that challenging objects require the right choice of the method (Ménétret et al., 2013), each having intrinsic limitations, but when combined these methods can create synergies at the interfaces that overcome the individual limits. For example, in X-ray crystallography a typical bottleneck is crystallisation, but it is not much restricted to a particular object size as illustrated by the possibility of crystallising small organic compounds and large complexes such as ribosomes and viruses (including very large viruses with a diameter in the 1000 Å range). However, in cryo-EM, a typical limitation is the lower size of a complex because the lower the molecular weight of the macromolecule the smaller the image contrast is, which limits the possibility of accurately determining the structure. Nevertheless, there are clear trends in the cryo-EM field to move towards smaller complexes. An example of this is our recent study of a 100 kDa complex, the first structure of a full-length nuclear receptor bound to an inverted DNA repeat, the USP/EcR complex in insects where EcR is the ecdysone receptor (Maletta et al., 2014); it revealed an asymmetric organisation of the complex although the DNA is almost symmetric (Figure 3); note that the data were collected at a reduced acceleration voltage (100 kV) to increase the image contrast. This represents a technical advance in the field with respect of studying relatively small complexes by cryo-EM, thus opening the possibility to study many other biological complexes and drug targets previously believed to be too small for cryo-EM. Other examples in the field are the studies of a 50 kDa RNA (Baird et al., 2010) and most recently the 3.8 Å resolution structure of a 93 kDa protein (Merk et al., 2016),

highlighting the fact that high-resolution structures can also be obtained on relatively small complexes, provided the biological samples behave well and can be imaged well (*i.e.* low aggregation, stability in relatively low-salt or low-detergent concentrations, good particle distribution etc.).

Among various structural biology methods that use averaging techniques, a common limitation is the sample homogeneity. While crystallisation (and re-crystallisation) can contribute to the high-level purification of a chemical compound or even a large macromolecular complex (*e.g.* PEG10000 precipitation of yeast and human ribosomes; Ben-Shem et al., 2010; Khatter et al., 2014; Khatter et al., 2015), sample homogeneity often limits crystallisation. However, the problem of sample heterogeneity can be turned into an advantage when using single-particle cryo-EM considering that with advanced image processing and 3D classification tools (see section Single particle cryo-EM analysis) different structures can be sorted and separated into distinct sub-populations, allowing to improve the refinement of a cryo-EM structure by local masking and refinement to high resolution and at the same time describe several conformational states of a complex that are in equilibrium with each other. Similarly, when using cryo-ET and sub-tomogram averaging of similar structures observed *in situ* in the cell (*e.g.* polyribosomes in Figure 2), it is possible to classify the aligned tomograms and address several structures at the same time (Heumann et al., 2011; Stölken et al., 2011; Frank et al., 2012; Kuybeda et al., 2013; Xu et al., 2013; Chen et al., 2014; Castaño-Díez et al., 2016; Obbineni et al., 2016). However, sorting is not possible on unique structures such as large regions of the cell, in which case methods such as focussed-ion beam/scanning electron microscopy (FIB/SEM) are more appropriate (*e.g.* chromatin in Figure 3; Orlov et al., 2015). FIB is a method originally emanating from material sciences, which, when applied to biological specimens, appears to be one of the most promising structural biology methods for future cell biology studies (Villa et al., 2013; Kizilyaprak et al., 2014; Rigort et al., 2015). In contrast to ultramicrotome sectioning of cells, which can exhibit knife cutting and compression artefacts, FIB milling allows obtaining high-quality cuts through the cell that can be observed by SEM (section by section to reconstitute a full tomogram, in the literal sense of τομός *tomos* (Greek: cut). Alternatively, thin lamella can be prepared by FIB milling and observed by cryo-ET (*e.g.* Mahamid et al., 2015; Schaffer et al., 2016; Zhang et al., 2016). Such analyses have the great advantage of being *in situ* (Lučič et al., 2013) and thus in the functional cellular context, but they require the identification of the complexes of interest by complementary methods such as fluorescence labelling. In an effort to allow the identification of chromatin structures, we have explored the possibilities of molecular imaging in cells through single-molecule localisation microscopy (SMLM; *e.g.* dSTORM, PALM; we used GSDIM, ground state depletion microscopy followed by individual molecule return). To make best use of super-resolution data, we developed an integrated software pipeline for image reconstruction, drift and chromatic aberration correction, co-localisation, resolution estimation, segmentation, clustering and quantification of labelled complexes (SharpViSu & ClusterViSu; Andronov et al., 2016a, 2016b). In addition to be very useful in the field of super-resolution microscopy, in the future such informatics tools may become particularly useful in the context of correlative light and electron microscopy (CLEM) approaches (Koning et al., 2014; Schirra et al., 2014; Arnold et al., 2016; Karreman et al., 2016; Schorb et al., 2016) to address the cellular fine structure, identify and localise protein complexes and visualise them at high resolution using cryo-EM and cryo-ET, that is perform an identification of the molecule-of-interest (MOI) rather than only the overall region-of-interest (ROI). Examples including SMLM (*e.g.* Kim et al., 2015) are studies of complexes such as RNA polymerase, nucleosomes, viruses or NPCs (Szymborska et al., 2013; Löschberger et al., 2014; Laine et al., 2015) some of which were reconstructed from super-resolution data using cryo-EM 3D reconstruction methods (Szymborska et al., 2013; Andronov et al., in prep.).

Current and near-future challenges in cryo-EM developments comprise key questions such as (i) how to push the resolution to the atomic level, (ii) how to analyse flexible complexes and (iii) how to integrate towards the cellular level. Two important areas to address these are (i) the instrumentation and (ii) software developments. Instrumentation (i) comprises for example high-resolution electron microscopes, direct electron detector cameras with higher DQE at high frequencies, energy filters to

remove inelastically scattered electrons and reduce the background in the images, correction of the spherical aberration (Cs) to improve the optical system in the column of the microscope, microelectron diffraction to determine the structure from small 3D crystals (Nederlof et al., 2013; Sawaya et al., 2016; Shi et al., 2016), spraying of small amounts on cryo-EM grids (Chen et al., 2015; Razinkov et al., 2016), cryo transfer between FIB and electron microscope for cryo-ET (Schaffer et al., 2016) and contrast-increasing phase plates placed in the back-focal plane of the microscope (Danev et al., 2014; Dai et al., 2014; Frindt et al., 2014; Walter et al., 2015; Chua et al., 2016; Danev et al., 2016; Glaeser, 2016; Rhinow 2016; Khoshouei et al., 2016a); phase plates could facilitate structure determination of relatively small complexes (Khoshouei et al., 2016b), which were difficult to address previously and usually limited to lower resolution (Baird et al., 2010; Orlov et al., 2012; Maletta et al., 2014) even though DDDs have helped a lot moving forward (Merk et al., 2016), suggesting that synergies will appear for example between phase plates, energy filters and high-sensitivity cameras to enable high-contrast high-resolution image acquisition (a feature that usually contradicts itself considering the requirement of defocussing during data collection to get some reasonable amount of image contrast required for image processing). Further software developments (ii) will be required for automatic data acquisition for massive data collection for single particle cryo-EM and cryo-ET (*e.g.* reviewed in Tan et al., 2016; automatic beam alignments including for Cs-corrected microscopes; remote control), and on-the-fly image processing during data collection, particle sorting and 3D classifications to address sample heterogeneity, automation in cryo-EM/cryo-ET structure determination, automation of backbone tracing like in X-ray crystallography, atomic model building and refinement into cryo-EM/cryo-ET maps of large macromolecular complexes to move towards larger cellular structures. Taken together, the scientific community is currently experiencing a very exciting era that is moving more and more towards the integration of various structural and imaging methods among which cryo-EM, cryo-ET and FIB will play a key role in multi-resolution integration. In close synergy with functional studies, this evolution towards cellular structural biology will lead in the coming years to unprecedented insights into cellular function and drug targets, including the analysis of the dynamic changes of macromolecular complexes that reflect their functional transitions in the cellular environment.

Funding

This work was supported by the European Research Council (ERC Starting Grant N_243296 TRANSLATIONMACHINERY), the Fondation pour la Recherche Médicale (FRM), the Association pour la Recherche sur le Cancer (ARC), the Alsace Region, the Agence National pour la Recherche, Université de Strasbourg and Investissement d'Avenir (IDEX), the Institut National du Cancer (INCa), the Centre National pour la Recherche Scientifique (CNRS), the Institut National pour la Recherche Médicale (Inserm), by the French Infrastructure for Integrated Structural Biology (FRISBI) ANR-10-INSB-05-01, and Instruct as part of the European Strategy Forum on Research Infrastructures (ESFRI).

Acknowledgements

We apologise to our colleagues for any publications not being cited which is due to space limitations and the cross-disciplinary nature of this review article. We would like to thank our colleagues with whom we collaborate on the projects mentioned in this review, notably Jean-Luc Vonesch, Alexander Spirin, Vladimir Shirokov, Dino Moras, Jean-François Peyron, Danièle Spehner and Christian Cambillau, and the members of our platforms and facilities for their support.

Conflict of interest statement

The authors have declared no conflict of interest.

References

Adams, P.D., Baker, D., Brunger, A.T., Das, R., DiMaio, F., Read, R.J., Richardson, D.C., Richardson, J.S. and Terwilliger, T.C. (2013) Advances, interactions, and future developments in the CNS, Phenix, and Rosetta structural biology software systems. Annu. Rev. Biophys. **42**, 265–287

Afonina, Z.A., Myasnikov, A.G., Shirokov, V.A., Klaholz, B.P. and Spirin, A.S. (2015) Conformation transitions of eukaryotic polyribosomes during multi-round translation. Nucleic Acids Res. **43**, 618–628

Afonina, Z.A., Myasnikov, A.G., Shirokov, V.A., Klaholz, B.P. and Spirin, A.S. (2014) Formation of circular polyribosomes on

eukaryotic mRNA without cap-structure and poly(A)-tail: a cryo electron tomography study. Nucleic Acids Res. **42**, 9461–9469

Afonine, P.V., Grosse-Kunstleve, R.W., Echols, N., Headd, J.J., Moriarty, N.W., Mustyakimov, M., Terwilliger, T.C., Urzhumtsev, A., Zwart, P.H. and Adams, P.D. (2012) Toward automated crystallographic structure refinement with phenix.refine. Acta Cryst. **D68**, 352–367

Allegretti, M., Mills, D.J., McMullan, G., Kühlbrandt, W. and Vonck, J. (2014) Atomic model of the F420-reducing [NiFe] hydrogenase by electron cryo-microscopy using a direct electron detector. Elife **3**:e01963. doi: 10.7554/eLife.01963.

Andronov, L., Lutz, Y., Vonesch, J.-L. and Klaholz, B.P. (2016a) SharpViSu: integrated analysis and segmentation of super-resolution microscopy data. Bioinformatics **32**, 2239–2241

Andronov, L., Orlov, I., Lutz, Y., Vonesch, J.-L. and Klaholz, B.P. (2016b) ClusterViSu, a method for clustering of protein complexes by Voronoi tessellation in super-resolution microscopy. Sci. Rep. **6**, 24084

Arnold, J., Mahamid, J., Lucic, V., de Marco, A., Fernandez, J.J., Laugks, T., Mayer, T., Hyman, A.A., Baumeister, W. and Plitzko, J.M. (2016) Site-Specific Cryo-focused Ion Beam Sample Preparation Guided by 3D Correlative Microscopy. Biophys. J. **110**, 860–869

Asano, S., Engel, B.D. and Baumeister, W. (2016) In Situ Cryo-Electron Tomography: A Post-Reductionist Approach to Structural Biology. J. Mol. Biol. **428**, 332–343

Bai, X.C., Fernandez, I.S., McMullan, G. and Scheres, S.H. (2013) Ribosome structures to near-atomic resolution from thirty thousand cryo-EM particles. eLife **2**:e00461. doi: 10.7554/eLife.00461.

Baird, N.J., Ludtke, S.J., Khant, H., Chiu, W., Pan, T. and Sosnick, T.R. (2010) Discrete structure of an RNA folding intermediate revealed by cryo-electron microscopy. J. Am. Chem. Soc. **132**, 16352–163523

Banerjee, S., Bartesaghi, A., Merk, A., Rao, P., Bulfer, S.L., Yan, Y., Green, N., Mroczkowski, B., Neitz, R.J., Wipf, P., Falconieri, V., Deshaies, R.J., Milne, J.L., Huryn, D., Arkin, M. and Subramaniam, S. (2016) 2.3 Å resolution cryo-EM structure of human p97 and mechanism of allosteric inhibition. Science **351**, 871–875

Barad, B.A., Echols, N., Wang, R.Y., Cheng, Y., DiMaio, F., Adams, P.D. and Fraser, J.S. (2015) EMRinger: side chain-directed model and **map** validation for 3D **cryo**-electron microscopy. Nat. Methods **12**, 943–946.

Beck, M., Förster, F., Ecke, M., Plitzko, J.M., Melchior, F., Gerisch, G., Baumeister, W. and Medalia, O. (2004) Nuclear pore complex structure and dynamics revealed by cryoelectron tomography. Science **306**, 1387–1390

Beinsteiner, B., Michalon, J. and Klaholz B. P. (2015) IBiSS, a versatile and interactive tool for integrated sequence and 3D structure analysis of large macromolecular complexes. Bioinformatics **31**, 3339–3344

Ben-Shem, A., Jenner, L., Yusupova, G. and Yusupov, M. (2010) Crystal structure of the eukaryotic ribosome. Science **330**, 1203–1209

Brandt, F., Carlson, L.A., Hartl, F.U., Baumeister, W. and Grünewald, K. (2010) The three-dimensional organization of polyribosomes in intact human cells. Mol. Cell **39**, 560–569

Briggs, J.A. (2013) Structural biology in situ - the potential of subtomogram averaging. Curr. Opin. Struct. Biol. **23**, 261–267

Brilot, A.F., Chen, J.Z., Cheng, A., Pan, J., Harrison, S.C., Potter, C.S., Carragher, B., Henderson, R. and Grigorieff, N. (2012) Beam-induced motion of vitrified specimen on holey carbon film. J. Struct. Biol. **177**, 630–637

Broennimann, C., Eikenberry, E.F., Henrich, B., Horisberger, R., Huelsen, G., Pohl, E., Schmitt, B., Schulze-Briese, C., Suzuki, M., Tomizaki, T., Toyokawa, H. and Wagner, A. (2006) The PILATUS 1M detector. J. Synchrotron Radiat. **13**, 120–130

Brown, A., Long, F., Nicholls, R.A., Toots, J., Emsley, P. and Murshudov, G. (2015) Tools for macromolecular model building and refinement into electron cryo-microscopy reconstructions. Acta Crystallogr. D Biol. Crystallogr. **71**, 136–153

Campbell, M.G., Cheng, A., Brilot, A.F., Moeller, A., Lyumkis, D., Veesler, D., Pan, J., Harrison, S.C., Potter, C.S., Carragher, B. and Grigorieff, N. (2012) Movies of ice-embedded particles enhance resolution in electron cryo-microscopy. Structure **20**, 1823–1828

Carazo, J.M., Sorzano, C.O., Otón, J., Marabini, R. and Vargas, J. (2015) Three-dimensional reconstruction methods in Single Particle Analysis from transmission electron microscopy data. Arch. Biochem. Biophys. **581**, 39–48

Carroni, M. and Saibil, H.R. (2016) Cryo electron microscopy to determine the structure of macromolecular complexes. Methods **95**, 78–85

Casanas, A., Warshamanage, R., Finke, A.D., Panepucci, E., Olieric, V., Nöll, A., Tampé, R., Brandstetter, S, Förster, A., Mueller, M., Schulze-Briese, C., Bunk, O. and Wang, M. (2016) EIGER detector: application in macromolecular crystallography. Acta Crystallogr. D Struct. Biol. **72**, 1036–1048

Castaño-Díez, D., Kudryashev, M. and Stahlberg, H. (2016) Dynamo Catalogue: Geometrical tools and data management for particle picking in subtomogram averaging of cryo-electron tomograms. J. Struct. Biol. **16**, 30111–30113

Chang, Y.W., Rettberg, L.A., Treuner-Lange, A., Iwasa, J., Søgaard-Andersen, L. and Jensen, G.J. (2016) Architecture of the type IVa pilus machine. Science **351**, 6278:aad2001

Chen, B., Kaledhonkar, S., Sun, M., Shen, B., Lu, Z., Barnard, D., Lu, T.M., Gonzalez, R.L. Jr. and Frank, J. (2015) Structural dynamics of ribosome subunit association studied by mixing-spraying time-resolved cryogenic electron microscopy. Structure **23**, 1097–1105

Chen, J.Z., Settembre, E.C., Aoki, S.T., Zhang, X., Bellamy, A.R., Dormitzer, P.R., Harrison, S.C. and Grigorieff, N. (2009) Molecular interactions in rotavirus assembly and uncoating seen by high-resolution cryo-EM. Proc. Natl. Acad. Sci. U.S.A. **106**, 10644–10648

Chen, Y., Pfeffer, S., Fernández, J.J., Sorzano, C.O. and Förster, F. (2014) Autofocused 3D classification of cryoelectron subtomograms. Structure **22**, 1528–1537

Chua, E.Y., Vogirala, V.K., Inian, O., Wong, A.S., Nordenskiöld, L., Plitzko, J.M., Danev, R. and Sandin, S. (2016) 3.9 Å structure of the nucleosome core particle determined by phase-plate cryo-EM. Nucleic Acids Res. **44**, 8013–8019

Dai, W., Fu, C., Khant, H.A., Ludtke, S.J., Schmid, M.F. and Chiu, W. (2014) Zernike phase-contrast electron cryotomography applied to marine cyanobacteria infected with cyanophages. Nat. Protoc. **9**, 2630–2642

Danev, R. and Baumeister, W. (2016) Cryo-EM single particle analysis with the Volta phase plate. Elife **5**: pii: e13046

Danev, R., Buijsse, B., Khoshouei, M., Plitzko, J.M. and Baumeister, W. (2014) Volta potential phase plate for in-focus phase contrast transmission electron microscopy. Proc. Natl Acad. Sci. U.S.A. **44**, 15635–15640

Dubochet, J., Adrian, M., Chang, J.J., Homo, J.C., Lepault, J., McDowall, A.W. and Schultz, P. (1988) Cryo-electron microscopy of vitrified specimens. Q. Rev. Biophys. **21**, 129–228

Dubrovsky, A., Sorrentino, S., Harapin, J., Sapra, K,T. and Medalia, O. (2015) Developments in cryo-electron tomography for in situ structural analysis. Arch. Biochem. Biophys. **581**, 78–85

Dudkina, N.V., Kouril, R., Bultema, J.B. and Boekema, E.J. (2010) Imaging of organelles by electron microscopy reveals protein-protein interactions in mitochondria and chloroplasts. FEBS Lett. **584**, 2510–2515

Earl, L.A. and Subramaniam, S. (2016) Cryo-EM of viruses and vaccine design. Proc. Nat. Acad. Sci. U.S.A. **113**, 8903–8905
Eiler, D., Lin, J., Simonetti, A., Klaholz, B.P. and Steitz, T.A. (2013) IF2 Initiation factor 2 crystal structure reveals a different domain organization from eukaryotic initiation factor 5B and mechanism among translational GTPases. Proc. Nat. Acad. Sci. U.S.A. **110**, 15662–15667
Emsley, P., Lohkamp, B., Scott, W.G. and Cowtan, K. (2010) Features and development of Coot. Acta Crystallogr. D Biol. Crystallogr. **66**, 486–501
Fischer, N., Konevega, A.L., Wintermeyer, W., Rodnina, M.V. and Stark, H. (2010). Ribosome dynamics and tRNA movement by time-resolved electron cryomicroscopy. Nature **466**, 329–333
Fischer, N., Neumann, P., Konevega, A.L., Bock, L.V., Ficner, R., Rodnina, M.V. and Stark, H. (2015) Structure of the E. coli ribosome-EF-Tu complex at $<$3 Å resolution by Cs-corrected cryo-EM. Nature **520**, 567–570
Frangakis, A.S., Böhm, J., Förster, F., Nickell, S., Nicastro, D., Typke, D., Hegerl, R. and Baumeister, W. (2002) Identification of macromolecular complexes in cryoelectron tomograms of phantom cells. Proc. Natl. Acad. Sci. U.S.A. **99**, 14153–14158
Frank, G.A., Bartesaghi, A., Kuybeda, O., Borgnia, M.J., White, T.A., Sapiro, G. and Subramaniam, S. (2012) Computational separation of conformational heterogeneity using cryo-electron tomography and 3D sub-volume averaging. J. Struct. Biol. **178**, 165–176
Frindt, N., Oster, M., Hettler, S., Gamm, B., Dieterle, L., Kowalsky, W., Gerthsen, D. and Schröder, R.R. (2014) In-focus electrostatic Zach phase plate imaging for transmission electron microscopy with tunable phase contrast of frozen hydrated biological samples. Microsc. Microanal. **1**, 175–183
Fu, J., Gao, H. and Frank, J. (2006) Unsupervised classification of single particles by cluster tracking in multi-dimensional space. J. Struct. Biol. **157**, 226–239
Galaz-Montoya, J.G., Hecksel, C.W., Baldwin, P.R., Wang, E., Weaver, S.C., Schmid, M.F., Ludtke, S.J. and Chiu, W. (2016) Alignment algorithms and per-particle CTF correction for single particle cryo-electron tomography. J. Struct. Biol. **194**, 383–394
Gao, H., Valle, M., Ehrenberg, M. and Frank, J. (2004) Dynamics of EF-G interaction with the ribosome explored by classification of a heterogeneous cryo-EM dataset. J. Struct. Biol. **147**, 283–290
Glaeser, R.M. (2016) Protein complexes in focus. Elife **5**: pii: e16156
Grant, T. and Grigorieff, N. (2015) Measuring the optimal exposure for single particle cryo-EM using a 2.6 Å reconstruction of rotavirus VP6. Elife **4**:e06980
Greber, B.J., Bieri, P., Leibundgut, M., Leitner, A., Aebersold, R., Boehringer, D. and Ban, N. (2015) The complete structure of the 55S mammalian mitochondrial ribosome. Science **348**, 303–308
Hagen, C., Dent, K.C., Zeev-Ben-Mordehai, T., Grange, M., Bosse, J.B., Whittle, C., Klupp, B.G., Siebert, C.A., Vasishtan, D., Bäuerlein, F.J., Cheleski, J., Werner, S., Guttmann, P., Rehbein, S., Henzler, K., Demmerle, J., Adler, B., Koszinowski, U., Schermelleh, L., Schneider, G., Enquist, L.W., Plitzko, J.M., Mettenleiter, T.C. and Grünewald, K. (2015) Structural Basis of Vesicle Formation at the Inner Nuclear Membrane. Cell **163**, 1692–1701
Hagen, W.J., Wan, W. and Briggs, J.A. (2016) Implementation of a cryo-electron tomography tilt-scheme optimized for high resolution subtomogram averaging. J. Struct. Biol. **16**, 30113–30117
Heumann, J.M., Hoenger, A. and Mastronarde, D.N. (2011) Clustering and variance maps for cryo-electron tomography using wedge-masked differences. J. Struct. Biol. **175**, 288–299
Irobalieva, R.N., Martins, B. and Medalia, O. (2016) Cellular structural biology as revealed by cryo-electron tomography. J. Cell Sci. **129**, 469–476
Karreman, M.A., Mercier, L., Schieber, N.L., Solecki, G., Allio, G., Winkler, F., Ruthensteiner, B., Goetz, J.G. and Schwab, Y. (2016) Fast and precise targeting of single tumor cells in vivo by multimodal correlative microscopy. J. Cell Sci. **129**, 444–456
Khatter, H., Myasnikov, A.G., Mastio, L., Billas, I.M.L., Birck C., Stella, S. and Klaholz, B.P. (2014) Purification, characterization and crystallization of the human 80S ribosome. Nucleic Acids Res. **42**, 1–11
Khatter, H., Myasnikov, A.G., Natchiar, K. and Klaholz, B.P. (2015) Structure of the human 80S ribosome. Nature **520**, 640–645
Khoshouei, M., Pfeffer, S., Baumeister, W., Förster, F. and Danev, R. (2016a) Subtomogram analysis using the Volta phase plate. J. Struct. Biol. **16**, 30103–30104
Khoshouei, M., Radjainia, M., Phillips, A.J., Gerrard, J.A., Mitra, A.K., Plitzko, J.M., Baumeister, W. and Danev, R. (2016b) Volta phase plate cryo-EM of the small protein complex Prx3. Nat. Commun. **7**, 10534
Kim, D., Deerinck, T.J., Sigal, Y.M., Babcock, H.P., Ellisman, M.H. and Zhuang, X. (2015) Correlative stochastic optical reconstruction microscopy and electron microscopy. PLoS One **10**, e0124581.
Kizilyaprak, C., Daraspe, J. and Humbel, B.M. (2014) Focused ion beam scanning electron microscopy in biology. J. Microsc. **254**, 109–114
Klaholz, B.P. (2015) Structure sorting of multiple macromolecular states in heterogeneous cryo-EM samples by 3D multivariate statistical analysis. Open J. Stat. **5**, 820–836
Klaholz, B.P., Myasnikov, A.G. and van Heel, M. (2004) Visualization of release factor 3 on the ribosome during termination of protein synthesis. Nature **427**, 862–865
Koning, R.I., Celler, K., Willemse, J., Bos, E., van Wezel, G.P. and Koster, A.J. (2014) Correlative cryo-fluorescence light microscopy and cryo-electron tomography of Streptomyces. Methods Cell Biol. **124**, 217–239
Kosinski, J., Mosalaganti, S., von Appen, A., Teimer, R., DiGuilio, A.L., Wan, W., Bui, K.H., Hagen, W.J., Briggs, J.A., Glavy, J.S., Hurt, E. and Beck, M. (2016) Molecular architecture of the inner ring scaffold of the human nuclear pore complex. Science **352**, 363–365
Kuijper, M., van Hoften, G., Janssen, B., Geurink, R., De Carlo, S., Vos, M., van Duinen, G., van Haeringen, B. and Storms, M. (2015) FEI's direct electron detector developments: Embarking on a revolution in cryo-TEM. J. Struct. Biol. **192**, 179–187
Kunath, W., Weiss, K., Sack-Kongehl, H., Kessel, M., Zeitler, E. (1984). Time-resolved low-dose microscopy of glutamine synthetase molecules. Ultramicroscopy **13**, 241–252
Kuybeda, O., Frank, G.A., Bartesaghi, A., Borgnia, M., Subramaniam, S. and Sapiro, G.A. (2013) Collaborative framework for 3D alignment and classification of heterogeneous subvolumes in cryo-electron tomography. J. Struct. Biol. **181**, 116–127
Laine, R.F., Albecka, A., van de Linde, S., Rees, E.J., Crump, C.M. and Kaminski, C.F. (2015) Structural analysis of herpes simplex virus by optical super-resolution imaging. Nat. Commun. **6**, 5980
Li, X., Mooney, P., Zheng, S., Booth, C.R., Braunfeld, M.B., Gubbens, S., Agard, D.A. and Cheng, Y. (2013) Electron counting and beam-induced motion correction enable near-atomic-resolution single-particle cryo-EM. Nat. Methods **10**, 584–590
Liao, H.Y., Hashem, Y. and Frank, J. (2015) Efficient estimation of three-dimensional covariance and its application in the analysis of heterogeneous samples in cryo-electron microscopy. Structure **23**, 1129–1237
Lin, D.H., Stuwe, T., Schilbach, S., Rundlet, E.J., Perriches, T., Mobbs, G., Fan, Y., Thierbach, K., Huber, F.M., Collins, L.N., Davenport, A.M., Jeon, Y.E. and Hoelz, A. (2016) Architecture of the symmetric core of the nuclear pore. Science **352**, 6283
Löschberger, A., Franke, C., Krohne, G., van de Linde, S. and Sauer, M. (2014) Correlative super-resolution fluorescence and electron microscopy of the nuclear pore complex with molecular resolution. J. Cell Sci. **127**, 4351–4355

Lučič, V., Rigort, A. and Baumeister, W. (2013) Cryo-electron tomography: the challenge of doing structural biology in situ. J. Cell Biol. **202**, 407–419

Lyumkis, D., Brilot, A.F., Theobald, D.L. and Grigorieff, N. (2013) Likelihood-based classification of cryo-EM images using FREALIGN. J. Struct. Biol. **183**, 377–388

Mahamid, J., Pfeffer, S., Schaffer, M., Villa, E., Danev, R., Cuellar, L.K., Förster, F., Hyman, A.A., Plitzko, J.M. and Baumeister, W. (2016) Visualizing the molecular sociology at the HeLa cell nuclear periphery. Science **351**, 969–972

Mahamid, J., Schampers, R., Persoon, H., Hyman, A.A., Baumeister, W. and Plitzko, J.M. (2015) A focused ion beam milling and lift-out approach for site-specific preparation of frozen-hydrated lamellas from multicellular organisms. J. Struct. Biol. **192**, 262–269

Maletta, M., Orlov, I.M., Roblin, P., Beck, Y., Moras, D., Billas, I.M.L. and Klaholz, B.P. (2014) The palindromic DNA-bound USP/EcR nuclear receptor adopts an asymmetric organization with allosteric domain positioning. Nat. Commun. **5**, 4139

McMullan, G., Chen, S., Henderson, R. and Faruqi, A.R. (2009) Detective quantum efficiency of electron area detectors in electron microscopy. Ultramicroscopy **109**, 1126–1143

McMullan, G., Faruqi, A.R., Clare, D. and Henderson, R. (2014) Comparison of optimal performance at 300keV of three direct electron detectors for use in low dose electron microscopy. Ultramicroscopy **147**, 156–163

Medalia, O., Weber, I., Frangakis, A.S., Nicastro, D., Gerisch, G. and Baumeister, W. (2002) Macromolecular architecture in eukaryotic cells visualized by cryoelectron tomography. Science **298**, 1209–1213

Ménétret, J-F., Khatter, H., Simonetti, A., Orlov, I., Myasnikov, A.G, Vidhya, K.V., Manicka, S., Torchy, M., Mohideen, K., Humm, A.-S., Hazemann, I., Urzhumtsev, A., Klaholz, B.P. (2013) Integrative structure-function analysis of large nucleoprotein complexes. In: D. Klostermeier and C. Hammann (Eds.). *RNA structure and folding*. de Gruyter.

Merk, A., Bartesaghi, A., Banerjee, S., Falconieri, V., Rao, P., Davis, M.I., Pragani, R., Boxer, M.B., Earl, L.A., Milne, J.L. and Subramaniam, S. (2016) Breaking Cryo-EM Resolution Barriers to Facilitate Drug Discovery. Cell **165**, 1698–1707

Milne, J.L., Borgnia, M.J., Bartesaghi, A., Tran, E.E., Earl, L.A., Schauder, D.M., Lengyel, J., Pierson, J., Patwardhan, A. and Subramaniam, S. (2013) Cryo-electron microscopy - a primer for the non-microscopist. FEBS J. **280**, 28–45

Murata, K., Liu, X., Danev, R., Jakana, J., Schmid, M.F., King, J., Nagayama, K. and Chiu, W. (2010) Zernike phase contrast cryo-electron microscopy and tomography for structure determination at nanometer and subnanometer resolutions. Structure **18**, 903–912

Myasnikov, A.G., Afonina, Z.A., Ménétret, J-F., Shirokov, V.A., Spirin, A.S. and Klaholz, B.P. (2014) The molecular structure of the left-handed supra-molecular helix of eukaryotic polyribosomes. Nat. Commun. **5**, 5294

Myasnikov, A.G., Afonina Z. and Klaholz, B.P. (2013) Single particle and molecular assembly analysis of polyribosomes by single- and double-tilt cryo electron tomography. Ultramicroscopy **126**, 33–39

Myasnikov, A.G., Natchiar, S.K., Nebout, M., Hazemann, I., Imbert, V., Khatter, H., Peyron, J-F. and Klaholz, B.P. (2016) Structure-function insights reveal the human ribosome as a cancer target for antibiotics. Nat. Commun. **7**, 12856

Nans, A., Kudryashev, M., Saibil, H.R. and Hayward, R.D. (2015) Structure of a bacterial type III secretion system in contact with a host membrane in situ. Nat. Commun. **6**, 10114

Nederlof, I., Li, Y.W., van Heel, M. and Abrahams, J.P. (2013) Imaging protein three-dimensional nanocrystals with cryo-EM. Acta Crystallogr. D Biol. Crystallogr. **69**, 852–859

Obbineni, J.M., Yamamoto, R. and Ishikawa, T. (2016) A simple and fast approach for missing-wedge invariant classification of subtomograms extracted from filamentous structures. J. Struct. Biol. **16**, 30172

Orlov, I., Rochel, N., Moras, D. and Klaholz, B.P. (2012) Structure of the full human RXR/VDR nuclear receptor heterodimer complex with its DR3 target DNA. EMBO J. **31**, 291–300

Orlov, I., Schertel, A., Zuber, G., Klaholz, B.P., Drillien, R., Weiss, E., Schultz, P. and Spehner, D. (2015) Live cell immunogold labelling of RNA polymerase II. Sci. Rep. **5**, 8324

Orlova, E.V. and Saibil, H.R. (2010) Methods for three-dimensional reconstruction of heterogeneous assemblies. Methods Enzymol. **482**, 321–41

Ortiz, J.O., Förster, F., Kürner, J., Linaroudis, A.A. and Baumeister, W. (2006) Mapping 70S ribosomes in intact cells by cryoelectron tomography and pattern recognition. J. Struct. Biol. **156**, 334–341

Penczek, P.A., Frank, J. and Spahn, C.M. (2006) A method of focused classification, based on the bootstrap 3D variance analysis, and its application to EF-G-dependent translocation. J. Struct. Biol. **154**, 184–194

Rajendran, C., Dworkowski, F.S., Wang, M. and Schulze-Briese, C. (2011) Radiation damage in room-temperature data acquisition with the PILATUS 6M pixel detector. J. Synchrotron Radiat. **18**, 318–328

Ray, P., Klaholz, B.P., Finn, R.D., Orlova, E.V., Burrows, P.C., Gowen, B., Buck, M. and van Heel, M. (2003) Determination of Escherichia coli RNA polymerase structure by single particle cryoelectron microscopy. Methods Enzymol. **370**, 24–42

Razinkov, I., Dandey, V.P., Wei, H., Zhang, Z., Melnekoff, D., Rice, W.J., Wigge, C., Potter, C.S. and Carragher, B. (2016) A new method for vitrifying samples for cryoEM. J. Struct. Biol. **195**, 190–198

Rhinow, D. (2016) Towards an optimum design for thin film phase plates. Ultramicroscopy **160**, 1–6

Rigort, A. and Plitzko, J.M. (2015) Cryo-focused-ion-beam applications in structural biology. Arch. Biochem. Biophys. **581**, 122–130

Ruskin, R.S., Yu, Z. and Grigorieff, N. (2013) Quantitative characterization of electron detectors for transmission electron microscopy. J. Struct. Biol. **184**, 385–393

Sawaya, M.R., Rodriguez, J., Cascio, D., Collazo, M.J., Shi, D., Reyes, F.E., Hattne, J., Gonen, T. and Eisenberg, D.S. (2016) Ab initio structure determination from prion nanocrystals at atomic resolution by MicroED. Proc. Natl. Acad. Sci. U.S.A. **2016**. pii: 201606287

Schaffer, M., Mahamid, J., Engel, B.D., Laugks, T., Baumeister, W. and Plitzko, J.M. (2016) Optimized cryo-focused ion beam sample preparation aimed at in situ structural studies of membrane proteins. J. Struct. Biol. **16**, 30151–30154

Scheres, S.H., Valle, M., Nuez, R., Sorzano, C.O., Marabini, R., Herman, G.T. and Carazo, J.M. (2005) Maximum likelihood multi-reference refinement for electron microscopy images. J. Mol. Biol. **22**, 139–149

Scheres, S.H. (2010) Classification of structural heterogeneity by maximum-likelihood methods. Methods Enzymol. **482**, 295–320

Scheres, S.H. (2014) Beam-induced motion correction for sub-megadalton cryo-EM particles. Elife **3**, e03665.

Schirra, R.T. Jr. and Zhang, P. (2014) Correlative fluorescence and electron microscopy. Curr. Protoc. Cytom. **70**, 1–10

Schorb, M., Gaechter, L., Avinoam, O., Sieckmann, F., Clarke, M., Bebeacua, C., Bykov, Y.S., Sonnen, A.F., Lihl, R. and Briggs, J.A. (2016) New hardware and workflows for semi-automated correlative cryo-fluoresence and cryo-electron microscopy/tomography. J. Struct. Biol. **16**, 30135–30136

Schur, F.K., Obr, M., Hagen, W.J., Wan, W., Jakobi, A.J., Kirkpatrick, J.M., Sachse, C., Kräusslich, H.G. and Briggs, J.A. (2016) An

atomic model of HIV-1 capsid-SP1 reveals structures regulating assembly and maturation. Science **353**, 506–508

Shi, D., Nannenga, B.L., de la Cruz, M.J., Liu, J., Sawtelle, S., Calero, G., Reyes, F.E., Hattne, J. and Gonen, T. (2016) The collection of MicroED data for macromolecular crystallography. Nat. Protoc. **11**, 895–904

Sigworth, F.J. (1998) A maximum-likelihood approach to single-particle image refinement. J. Struct. Biol. **122**, 328–339

Simonetti, A., Marzi, S., Fabbretti, A., Hazemann, I., Jenner, L., Urzhumtsev, A., Gualerzi, C.O. and Klaholz, B.P. (2013a) Structure of the protein core of translation initiation factor 2 in apo, GTP-bound and GDP-bound forms. Acta Cryst. **D69**, 925–933

Simonetti, A., Marzi, S., Billas, I.M.L., Tsai, A., Fabbretti, A., Myasnikov, A.G., Roblin, P., Vaiana, A.C., Hazemann, I., Eiler, D., Steitz, T.A., Puglisi, J.D., Gualerzi, C.O. and Klaholz, B.P. (2013b) Involvement of IF2 N domain in ribosomal subunit joining revealed from architecture and function of the full-length initiation factor. Proc. Nat. Acad. Sci. U.S.A. **110**, 15656–15661

Simonetti, A., Ménétret, J-F., Martin, F., Myasnikov, A.G., Vicens, Q., Prongidi-Fix, L., Natchiar, S.K., Klaholz, B.P. and Eriani, G. (2016) Ribosomal 18S rRNA base pairs with mRNA during eukaryotic translation initiation. Nat. Commun. **7**, 12622

Simonetti, A., Marzi, S., Myasnikov, A.G., Fabbretti, A., Yusupova, G., Yusupov, M., Gualerzi, C.O. and Klaholz, B.P. (2008) Structure of the 30S translation initiation complex. Nature **455**, 416–420

Smart, O.S., Womack, T.O., Flensburg, C., Keller, P., Paciorek, W., Sharff, A., Vonrhein, C. and Bricogne, G. (2012) Exploiting structure similarity in refinement: automated NCS and target-structure restraints in BUSTER. Acta Crystallogr. D Biol. Crystallogr. **68**, 368–380

Sobolev, O.V., Afonine, P.V., Adams, P.D. and Urzhumtsev, A. (2015) Programming new geometry restraints: parallelity of atomic groups. J. Appl. Crystallogr. **48**, 1130–1141

Spear, J.M., Noble, A.J., Xie, Q., Sousa, D.R., Chapman, M.S. and Stagg, S.M. (2015) The influence of frame alignment with dose compensation on the quality of single particle reconstructions. J. Struct. Biol. **192**, 196–203

Spinelli, S., Bebeacua C., Orlov, I., Tremblay, D., Klaholz, B.P., Moineau, S. and Cambillau, C. (2014) CryoEM structure of the lactococcal siphophage 1358 virion. J. Virol. **88**, 8900–8910

Stölken, M., Beck, F., Haller, T., Hegerl, R., Gutsche, I., Carazo, J.M., Baumeister, W., Scheres, S.H. and Nickell, S. (2011) Maximum likelihood based classification of electron tomographic data. J. Struct. Biol. **173**, 77–85

Szymborska, A., de Marco, A., Daigle, N., Cordes, V.C., Briggs, J.A. and Ellenberg, J. (2013) Nuclear pore scaffold structure analyzed by super-resolution microscopy and particle averaging. Science **341**, 655–658

Tan, Y.Z., Cheng, A., Potter, C.S. and Carragher, B. (2016) Automated data collection in single particle electron microscopy. Microscopy (Oxf.) **65**, 43–56

van Heel, M., Gowen, B., Matadeen, R., Orlova, E.V., Finn, R., Pape, T., Cohen, D., Stark, H., Schmidt, R., Schatz, M. and Patwardhan, A. (2000) Single-particle electron cryo-microscopy: towards atomic resolution. Q. Rev. Biophys. **33**, 307–369

Veesler, D., Campbell, M.G., Cheng, A., Fu, C.Y., Murez, Z., Johnson, J.E., Potter, C.S. and Carragher, B. (2013) Maximizing the potential of electron cryomicroscopy data collected using direct detectors. J. Struct. Biol. **184**, 193–202

Villa, E., Schaffer, M., Plitzko, J.M. and Baumeister, W. (2013) Opening windows into the cell: focused-ion-beam milling for cryo-electron tomography. Curr. Opin. Struct. Biol. **23**, 771–777

Walter, A., Steltenkamp, S., Schmitz, S., Holik, P., Pakanavicius, E., Sachser, R., Huth, M., Rhinow, D. and Kühlbrandt, W. (2015) Towards an optimum design for electrostatic phase plates. Ultramicroscopy **153**, 22–31

Wan, W. and Briggs, J.A. (2016) Cryo-electron tomography and subtomogram averaging. Methods Enzymol. **579**, 329–367

Wang, K., Fu, C.Y., Khayat, R., Doerschuk, P.C. and Johnson, J.E. (2011) In vivo virus structures: simultaneous classification, resolution enhancement, and noise reduction in whole-cell electron tomography. J. Struct. Biol. **174**, 425–433

White, H.E., Saibil, H.R., Ignatiou, A. and Orlova, E.V. (2004) Recognition and separation of single particles with size variation by statistical analysis of their images. J. Mol. Biol. **13**, 453–460

Wong, W., Bai, X.C., Brown, A., Fernandez, I.S., Hanssen, E., Condron, M., Tan, Y.H., Baum, J. and Scheres, S.H. (2014) Cryo-EM structure of the Plasmodium falciparum 80S ribosome bound to the anti-protozoan drug emetine. Elife **3**. doi: 10.7554/eLife.03080

Xu, M. and Alber, F. (2013) Automated target segmentation and real space fast alignment methods for high-throughput classification and averaging of crowded cryo-electron subtomograms. Bioinformatics **29**, 274–282

Yang, Z., Lasker, K., Schneidman-Duhovny, D., Webb, B., Huang, C.C., Pettersen, E.F., Goddard, T.D., Meng, E.C., Sali, A. and Ferrin, T.E. (2012) UCSF Chimera, MODELLER, and IMP: an integrated modeling system. J. Struct. Biol. **179**, 269–278

Zhang, J., Ji, G., Huang, X., Xu, W. and Sun, F. (2016) An improved cryo-FIB method for fabrication of frozen hydrated lamella. J. Struct. Biol. **194**, 218–223

Zhang, X., Ge, P., Yu, X., Brannan, J.M., Bi, G., Zhang, Q., Schein, S. and Zhou, Z.H. (2013) Cryo-EM structure of the mature dengue virus at 3.5-Å resolution. Nat. Struct. Mol. Biol., **20**, 105–110

Received: 12 July 2016; Revised: 4 October 2016; Accepted: 5 October 2016; Accepted article online: 12 October 2016